Impact of sea ice on air-sea CO_2 exchange – a critical review of polar eddy covariance studies

Jennifer Watts[1*], Thomas G. Bell[2], Karen Anderson[3], Brian J. Butterworth[4], Scott Miller[5], Brent Else[6], Jamie Shutler[1]

[1]Centre for Geography and Environmental Science, University of Exeter, Penryn, Cornwall, UK.

[2]Plymouth Marine Laboratory, Plymouth, Devon, UK.

[3]Environment and Sustainability Institute, University of Exeter, Penryn, Cornwall.

[4]University of Wisconsin-Madison, Madison, Wisconsin, USA.

[5]Atmospheric Sciences Research Centre, University of Albany (State University of New York), USA.

[6]Department of Geography, University of Calgary, Canada.

*Corresponding author: Jennifer Watts (j.h.watts@exeter.ac.uk)

Keywords: 'air-sea gas exchange', 'gas transfer velocity', 'air-sea carbon-dioxide fluxes' 'eddy covariance', 'remote sensing', 'sea ice'

Abstract

Sparse *in situ* measurements and poor understanding of the impact of sea ice on air-sea gas exchange introduce large uncertainties to models of polar oceanic carbon uptake. The eddy covariance technique can be used to produce insightful air-sea gas exchange datasets in the presence of sea ice, but results differ between studies. We present a critical review of historical polar eddy covariance studies and can identify only five that present comparable flux datasets. Assessment of ancillary datasets, including sea-ice coverage and type and air-sea concentration gradient of carbon dioxide, used to interpret flux datasets (with a specific focus on their role in estimating and interpreting sea ice zone gas transfer velocities) identifies that standardised methodologies to characterise the flux footprint would be beneficial. In heterogeneous ice environments both ancillary data uncertainties and controls on gas exchange are notably complex. To address the poor understanding, we highlight how future efforts should focus on the collection of robust gas flux datasets within heterogeneous sea ice regions during key seasonal processes alongside consistent ancillary data with a full characterisation of their associated uncertainties.

1 Introduction

The ocean absorbs ~25% of all anthropogenic carbon dioxide (CO_2) emitted annually (Friedlingstein *et al*., 2020), mediating the impacts of anthropogenic climate change whilst driving ocean acidification (Clarke *et al.*, 2017; Gao *et al.*, 2012; Gattuso *et al.*, 2015). Accurate estimates of this oceanic carbon sink are essential for balancing global and regional carbon budgets (Shutler et al., 2020) and carbon uptake in the polar oceans is an important component of the global oceanic total. The Arctic Ocean is estimated to be responsible for 5 – 15% of the total oceanic uptake (Bates and Mathis, 2009; MacGilchrist et al., 2014; Yasunaka et al., 2016) and the Southern Ocean for 40% (Caldeira and Duffy, 2000; Devries, 2014; Mikaloff Fletcher et al., 2006). However, large uncertainties in these polar estimates exist due to sparse polar measurements and the poorly understood influence of sea ice on air-sea gas exchange (Prytherch and Yelland, 2021).

Understanding the impact of sea ice on air-sea gas exchange is becoming increasingly important as the polar oceans respond to climate change. Strong Arctic amplification of global warming (Serreze and Barry, 2011) means Arctic sea ice is rapidly becoming thinner, with reduced coverage (Kwok, R. and Rothrock, 2009; Kwok, Ronald and Untersteiner, 2011; Meier *et al.*, 2007; Serreze and Stroeve, 2015; Stroeve *et al*, 2012). As Arctic sea ice retreats, the width of the Arctic marginal ice zone (MIZ) is increasing (Strong and Rigor, 2013). In the Southern Ocean, climatic changes are modulating sea-ice extent (Parkinson, 2019), driving major shifts in the seasonality of sea ice (Stammerjohn *et al.*, 2008) and an increase in storminess (e.g. Lubin *et al.*, 2008). Storms amplify wave-ice interaction, with potential impacts on pancake ice formation, ice fragmentation and MIZ width (Massom and Stammerjohn, 2010). At both Poles, shifts in the sea-ice regime are influencing ice-ocean-atmosphere interactions and air-sea gas exchange.

The exchange of CO_2 across the air-water interface can occur in either direction, depending on the air-sea concentration difference. Woolf *et al.* (2016) define the bulk air-sea gas flux as:

$$F_i = K_i (C_i - C_M), \quad (1)$$

where F_i is the vertical flux of CO_2 to/from the sea surface, K_i is the interfacial gas transfer velocity (herein referred to as K), C_i is the interfacial CO_2 concentration and C_M is the CO_2 concentration at the base of the ocean molecular boundary layer. The ocean molecular boundary layer is the thin layer at the ocean surface over which gradients of mass concentration associated with an air-sea disequilibrium are confined (Woolf *et al.*, 2016). The CO_2 concentration is the product of the partial pressure of CO_2 (ρCO_2) and solubility, which is predominantly temperature dependent (Woolf *et al*, 2016). K is the inverse of the resistance to gas transfer across the air-sea interface, and thus describes the efficiency of gas exchange (Liss and Slater, 1974). Air-sea CO_2 fluxes are influenced by factors that alter the air-sea concentration difference of CO_2 and/or K (Figure 1). The bulk flux equation (Eqn. 1) is used to estimate net air-sea CO_2 fluxes scales (regional to global, daily to annual) required to constrain the global carbon budget. At present these are estimated to have a total global average uncertainty of ± 20% (Woolf *et al.* 2019).

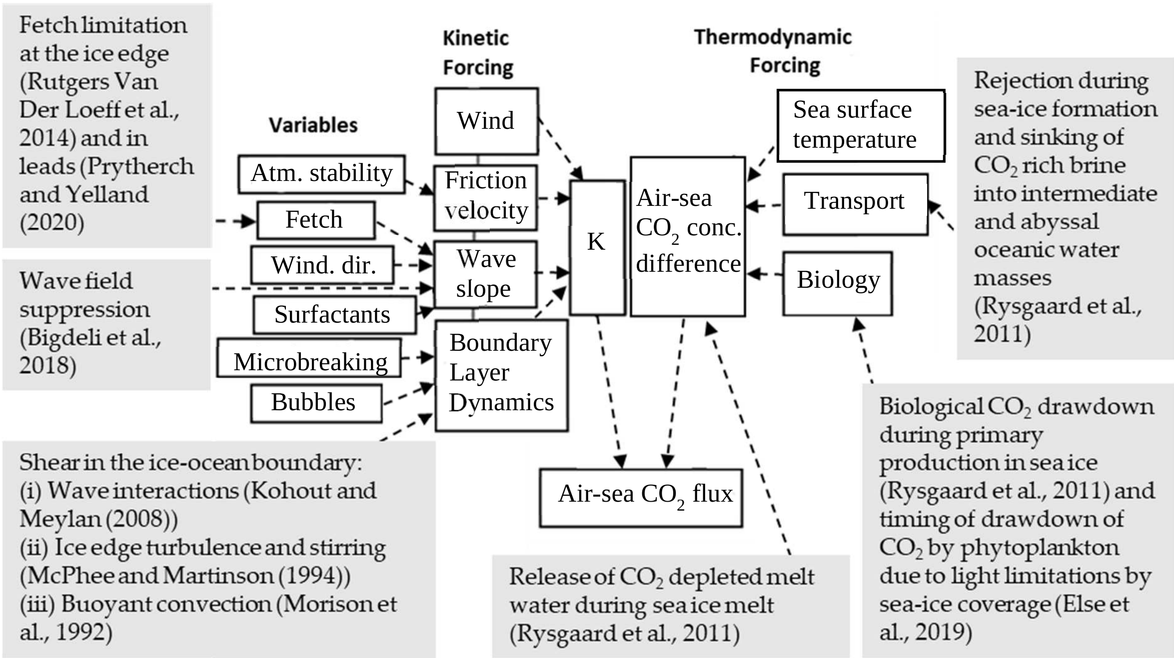

Figure 1. Summary of air-sea gas exchange controls adapted from Wanninkhof *et al.* (2009) to include sea ice-relevant processes from the literature (grey shaded boxes).

Uncertainty in K is considered to be the dominant source of uncertainty within global air-sea CO_2 flux estimates (Woolf *et al*, 2016). Wind speed is the primary physical force that drives near surface ocean turbulence and is thus the proxy used most often to parameterise open ocean K (Ho *et al.*, 2011; Shutler *et al.*, 2019; Wanninkhof, 2014). Existing parameterisations of K are typically empirically derived functions of horizontal wind speed at a height of 10 m (Wanninkhof, 2014; Lovely *et al.*, 2015). However, there is evidence that a single wind speed parameterisation cannot adequately parameterise the gas transfer velocity for all oceanic conditions (Shutler *et al.*, 2020; Wanninkhof *et al.*, 2009). Specific examples from the literature are gas transfer velocity in estuarine/fjord environments (Banko-Kubis et al., 2019), conditions where wave breaking is driving bubble mediated gas transfer (Deike and Melville, 2018) or gas transfer velocity in the presence of surfactants (Pereira et al., 2018).

Wind speed-derived K in the sea-ice zone is often scaled to the fraction of open water (Stephens and Keeling, 2000; Arrigo and Van Dijken, 2007; Takahashi *et al.*, 2009; Loose *et al.*, 2014; Shutler *et al*., 2016) . This assumes that all types of ice coverage at all times of year act as a complete barrier to gas exchange (Arrigo and Van Dijken, 2007; Stephens and Keeling, 2000; Takahashi *et al.*, 2009), and that boundary layer dynamics in the open water portions of the icescape respond to wind forcing the same as in the open ocean. A simple linear scaling of K to sea ice concentration (SIC) offers a first approach, but has had limited evaluation in the field. Collated information from the literature on sea-ice processes relevant to gas exchange controls (Figure 1) highlights that the relationship between sea ice and air-sea gas exchange controls is complex, particularly in mixed ice-water environments. Evidence has been presented that suggests sea ice, and ice-water interactions, can either inhibit (Bigdeli et al., 2018; Butterworth and Miller, 2016a; Prytherch et al., 2017; Rutgers Van Der Loeff et al., 2014) or enhance (Kohout and Meylan, 2008; Loose et al., 2017; McPhee and Martinson, 1994; Morison et al., 1992) gas exchange. The mismatch between practical applications of the impact of sea ice on gas exchange (e.g. the linear scaling method) and evidence from the literature drives a need for field-techniques that can make observations of gas exchange at scales compatible with improving K parameterisations for complex mixed ice-water environments.

Eddy covariance is a micrometeorological method used to quantify air-sea CO_2 fluxes using the covariance of rapid fluctuations in atmospheric gas concentrations and vertical wind velocities (Blomquist *et al.*, 2014; Miller, S. *et al.*, 2010). K can be in-directly estimated from eddy covariance air-sea CO_2 flux datasets by rearranging the bulk flux equation (Eqn.1) if solubility and CO_2 concentrations are also measured. Eddy covariance results are time-averaged (order of 20 – 180 minutes) and represent vertical fluxes from a 'source area' or 'flux footprint' upwind of the sensor (order of 100 m – 1 km). It should also be noted that eddy covariance is not the only field technique for studying gas exchange processes in the presence of sea ice, there is also the radon-deficiency method (a mass balance method), which also provides an indirect estimate of K (e.g. Rutgers Van Der Loeff *et al.*, 2014; Loose *et al.*, 2017) and the enclosure method which has been used to measure gas fluxes through ice (e.g. Geilfus *et al.*, 2014). While heterogeneous conditions present an inherent challenge (Bell et al., 2015; Hill et al., 2017) the ability of eddy covariance to capture data at temporal and spatial scales that encompass the natural heterogeneity of sea-ice and mixed ice-water environments is a major advantage over the enclosure (< 1 m, > 12 hours) and radon-deficit methods (3-4 days, > 10 km) (Butterworth and Else, 2018). The temporal and spatial scales of eddy covariance datasets means they can be used to study process-level variability in air-sea gas exchange, which in turn helps to determine which processes are relevant to estimates of regional to global air-sea fluxes made using the bulk flux equation (Eqn. 1). Improvements in eddy covariance methods that identify and reduce the uncertainties in these measurements are likely to increase the reconciliation between all the methodologies commonly used to study air-sea gas exchange, both fluxes and gas transfer velocity, and the oceanic carbon sink.

The eddy covariance technique has evolved considerably over the timeframe of the polar marine eddy covariance studies identified in this work (2004 – 2020) both as a result of the experimental set-up and post-processing techniques used to produce reliable measurements (see

Dong *et al.*, 2021; Landwehr *et al.*, 2015). To ascertain the current state of knowledge we present a critical review of the identified studies to address the following research questions:

1. **Can the results of historical polar eddy covariance studies of air-sea/air-ice-sea** CO_2 **fluxes be objectively compared?** We reviewed the study systems, methodologies and results of historical polar eddy covariance studies of CO_2 flux in regions of partial to full sea-ice coverage and placed their results in the context of recent advances in knowledge in the field.

2. **What are key sources of uncertainty in the interpretation of polar eddy covariance flux datasets?** Linked to the comparison of historical studies the review compared the usage, and associated uncertainties, of key ancillary datasets (e.g. air-sea concentration gradient of CO_2 and sea-ice data used for flux footprint characterisation).

3. **Where should future effort to understand polar air-sea gas exchange of** CO_2 **using eddy covariance be focussed?** Using the findings of the review process we identified focus areas for future studies.

2 Materials and Methods

Papers that present air-sea fluxes of CO_2 in sea-ice environments measured using eddy covariance were collated using a literature search in Google Scholar. The search used the key terms 'eddy covariance', 'polar oceans', 'sea ice', 'CO_2 fluxes', 'gas fluxes', 'gas transfer velocity', 'air-sea gas fluxes', 'air-sea carbon-dioxide fluxes', 'air-sea gas exchange', 'Arctic', 'Antarctic', 'Southern Ocean'. Results were filtered to only include CO_2 fluxes measured using the eddy covariance technique in the Arctic or Southern Ocean in the presence of partial to full sea ice cover. The 'snowballing technique' was applied to identify any other relevant work, which uses the references of the papers identified in the search to identify further relevant titles for investigation (Creswell & Poth, 2016). Twelve papers were identified that met all the criteria.

3 Review of eddy covariance studies of air-sea exchange of CO_2 in sea-ice regions

Key information on the study system, experimental set-up and conclusions of the twelve identified polar eddy covariance studies is presented in Table 1. There are ten studies in the Arctic which include flux measurements made over landfast sea ice during spring melt season (Semilet*ov et al.*, 2004, 2007; Miller, Papakyriakou, *et al.*, 2011; Papakyriakou and Miller, 2011; Butterworth and Else, 2018), over-winter in an active polynya (Els*e et al.*, 2011), in the Arctic MIZ through mid-summer to autumn (Prytherch et al., 2017) and over central Arctic Ocean pack-ice during summer (Prytherch and Yelland, 2021). In the Antarctic there are only two published studies, the first measured CO_2 fluxes over multiyear ice in the Weddell Sea (Zemmelink et al., 2006) and the second measured CO_2 fluxes over the Southern Ocean and Antarctic MIZ through spring to summer (Butterworth and Miller, 2016b). Gas transfer velocity estimates are presented in three of these studies: Prytherch *et al.* (2017) in the Arctic MIZ; Butterworth and Miller (2016a) in the Antarctic MIZ; and Prytherch and Yelland (2021) over leads within central Arctic pack ice.

There are clear disparities in the study system, methodology and results of the identified studies (Table 1). Earlier studies have tended to conclude sea ice as an active component of the carbon cycle in a range of ice regimes. This includes observations of air-ice exchange over winter (Miller, Papakyriakou, *et al.*, 2011), enhanced uptake over sea ice with melt ponds and through brine channels during spring melt season (Miller, L. A., Papakyriakou, *et al.*, 2011; Papakyriakou and Miller, 2011; Semiletov *et al.*, 2004, 2007) and enhanced exchange during active sea-ice formation (Else et al., 2011). Studies in both the Arctic MIZ (Prytherch *et al.*, 2017) and Antarctic MIZ (Butterworth and Miller, 2016b) have presented evidence to suggest that it is reasonable to linearly scale K with SIC. Conversely, Prytherch & Yelland (2021) present evidence that K is supressed by 30% (compared to typical open-ocean parameterisations) within sea-ice leads. A table synthesising the full detailed methodology of each study is presented in supplementary materials (Table S1).

Table 1. Overview of polar air-sea CO_2 flux study sites and results. Shaded rows indicate when closed-path gas analysers were used.

Study	***Platform/ location***	***Dates***	***Season/ice conditions***	***Gas analyser***	***Findings/conclusions***
Semiletov *et al.* (2004)	Land-based tower, Point Barrow, Arctic	06/06/2002 to 24/06/2002	Late Spring, Melting landfast ice	Not stated	Sea-ice melt ponds and open brine channels form an important CO_2 sink during spring/summer melt season.
Zemmelink *et al.* (2006)	Drift station on ice floe, Weddell Sea, Antarctica	37 days in November – December 2004	Early summer, Multiyear ice	Open-path Li-Cor 7500	Uptake of CO_2 over snow covered multi-year sea ice of between -18.2 to -4.5 mmol m^{-2} d^{-1} driven by biological activity at the ice-snow interface.
Semiletov *et al.* (2007)	Land-based tower, Coastal zone of the Chukchi Sea	September 2005	Mid-Spring, Melting landfast ice	Open-path Li-Cor 7500	Sea-ice melt ponds and open brine channel form important CO_2 sink during spring/summer melt season.
Else *et al.* (2011)	Ship-mounted, Arctic Polynya	01/11/2007 to 31/01/2008	Mid-winter, Active polynya	Open-path Li-Cor 7500	Enhanced air-sea gas exchange in mixed ice environments during ice formation.
Miller *et al.* (2011)	Land-based tower, Beaufort Sea	22/01/2004 to 25/05/2004	Winter to late Spring, Landfast ice (coldest	Open-path Li-Cor 7500	Sea ice is an active participant in the carbon cycle.

			period into spring melt)		
Papakyriakou & Miller (2011)	Tower mounted on ice, Canadian Arctic Archipelago	09/05/2002 to 24/06/2002	Spring, Seasonal landfast ice	Open-path Li-Cor 7500	High CO_2 fluxes (maximum efflux = 1, maximum uptake = -259.2 mmol m^{-2} d^{-1}) over seasonal landfast sea ice comparable with fluxes over land.
Sørensen et al. (2014)	Tower mounted in ice, Greenlandic fjord	12/03/2010 to 16/03/2010	Seasonal landfast ice	Open-path Li-Cor 7500	Air-ice fluxes between −244.5 to 86.4 mmol m^{-2} d^{-1}. Study proposes use of conceptual model for calculation of air–sea ice fluxes based on the resistance analogy
Sievers *et al.* (2015)	Ice mounted towers, Greenlandic fjord	20 – 27th March 2012 (ICE1) 29th March – 27th April 2012 (DNB), 25th to 27th March 2012 (POLY1).	Early March to late April, two landfast ice sites and a newly formed polynya	Open-path Li-Cor 7500	Outgassing (8.64 ±3 9.64 mmol m^{-2} day^{-1}) over one landfast ice site and uptake over the polynya (−9.9 7± 19.8 mmol m^{-2} day^{-1})
				Closed-path Li-Cor 7200	Outgassing (1.73 ± 5 mmol m^{-2} day^{-1}) with the progression of spring time warming and strong winds.
Butterworth & Miller (2016a)	Ship-mounted, Southern Ocean and Antarctic MIZ	Cruise 1 (NBP-1210): 01/01/2013 to 08/02/2013 Cruise 2 (NBP-1402): 29/01/2014 to 15/03/2014	Mid-summer through to early autumn, Antarctic MIZ	Closed-path Li-Cor 7200	Gas transfer velocity scales linearly with sea ice concentration in the MIZ.
Prytherch *et al.* (2017)	Ship-mounted, Arctic	05/07/2014 to 05/10/2014	Mid-summer to Autumn,	Los Gatos Fast	Gas transfer velocity scales linearly with sea

	Ocean MIZ		Arctic MIZ	Greenho use Gas Analyser	ice concentration in the MIZ.
Butterworth & Else (2018)	Land-based tower, Amunsden Gulf, Arctic	04/05/2017 to 01/09/2017	Landfast ice during Spring melt season	Closed-path Li-Cor 7200	Air-drying combined with closed path infrared gas analysers can reconcile eddy covariance and enclosure measured fluxes over landfast sea ice.
Prytherch & Yelland (2021)	Drift station on ice floe, Central Arctic Ocean		Late Summer to Early Autumn, Dense pack ice with lead systems	Closed-path Li-Cor 7200	Wind-speed dependent gas transfer velocity is supressed by 25-30% in leads relative to the open ocean.

3.1 Closed-path gas analysers and sample drying

Eddy covariance requires high precision measurements of atmospheric CO_2 fluctuations. Open-path infrared gas analysers (IRGAs) produce unreliable results in marine environments due to biases driven by cross-sensitivities to water vapour *(Blomquist et al.*, 2014; Kohsiek, 2000; Miller, S. *et al.*, 2010), which cannot be satisfactorily corrected for using post-hoc corrections (e.g. the WPL correction is too large for use in low flux environments (Jentzsch, Boike, & Foken, 2021); and the PKT correction is ineffective (Landwehr, Miller, Smith, Saltzman, & Ward, 2014)). This has significant consequences for earlier studies in which open-path gas analysers were used (see Table 1) prior to the identification of these instrument biases. The effect of open-path gas analysers is visible in these studies through the reporting of highly variable CO_2 fluxes in sea-ice regions, often including fluxes higher than typical open ocean values (Else et al., 2011; Miller et al., 2011b; Papakyriakou and Miller, 2011; Semiletov et al., 2007, 2004; Zemmelink et al., 2006). The lead authors of Else *et al.* (2011), Miller *et al.* (2011) and Papakyriakou and Miller (2011) (L. Miller, T.Papkyriakou, personal communication via email, 11th September 2019) have confirmed that they do not consider the data produced in these studies to be as reliable as the measurements reported in more recent work.

More recent eddy covariance air/sea CO_2 flux measurements have made substantial progress through the use of closed path systems that eliminate water vapour fluctuations (Blomquist *et al.*, 2014). Drying sample air substantially reduces the water vapour in the sample, removes the water vapour fluctuations and dramatically reduces the magnitude of associated corrections (Butterworth and Else, 2018; Miller, S. *et al.*, 2010; Webb *et al.*, 1980). Comparison between dried and undried cavity ring down spectrometer (CRDS) flux measurements has also demonstrated that a numerical correction for mean water vapour content can be sufficient to yield accurate CO_2 fluxes when combined with a closed path setup (Yang *et al.*, 2016). The authors demonstrated that a closed path system (i.e. sample air pulled through a length of tubing into the analyser) effectively eliminates the high frequency water vapour fluctuations that would otherwise affect the measured CO_2 flux. Closed path measurements made on dried air samples are presented in Sievers *et al.*, (2015), Butterworth and Miller (2016a), Butterworth and Else (2018). Prytherch and Yelland (2021) used a closed path, Li-Cor with an undried sample but considered conditions to be sufficiently dry during the study period. Prytherch *et al.* (2017) used a closed path Los Gatos Research Fast Greenhouse Gas Analyser (a Cavity Ringdown Spectrometer) with an undried air sample and numerical water vapour correction. Gas transfer velocity estimates from closed path flux systems operated in open ocean environments now yield results that are typically within 20% of other tracer-based estimates and can be used to investigate the small scale variability in K (Bell et al., 2017; Blomquist et al., 2017; Butterworth and Miller, 2016b; Dong et al., 2021b; Landwehr et al., 2018; Miller et al., 2009; Yang et al., 2021; Zavarsky et al., 2018).

3.2 Modelling the location of the flux footprint

The flux footprint position relative to the eddy covariance measurement location is determined by the wind direction, while footprint extent (distance from the measurement point that flux signals can be observed) is predominantly a function of measurement height as well as aerodynamic surface roughness, horizontal wind speed and atmospheric stability (Kljun *et al.*, 2015). The parameters required to estimate the flux footprint location and extent, can be determined from measurements made at the eddy covariance tower. However, it should be noted that sea ice characteristics (e.g. ice age, ice type, melt ponds, snow cover) will also impact the aerodynamic roughness length of sea ice (Andreas *et al.*, 2010; Guest and Davidson, 1991; Smeets and Broeke, 2008; Weiss *et al.*, 2011) and thus the flux footprint extent.

There has been limited evaluation of the spatial and temporal resolution of eddy covariance flux footprints in sea-ice regions and no comparison with the spatial resolution of concurrent sea ice and oceanic condition measurements. Of the studies in Table 1, only two studies present evidence of modelling the flux footprint. Butterworth and Else (2018) use the Kljun *et al.* (2015) flux footprint prediction model to exclude fluxes that had been influenced by land. Prytherch and Yelland (2021) evaluated the flux footprint estimation and its impact on the interpretation of their flux dataset. The authors used two models (Kljun *et al.* (2015); Hsieh *et al.* (2000)) to directly compare the CO_2 flux footprint with measurements of the lead dimensions. The relative proportions of water and ice in the footprint were determined with high precision using both models. Estimates of K were found to be sensitive to the model used to determine the open water fraction, however it was not possible to determine which footprint model is most accurate in regions with sea ice (Prytherch and Yelland, 2021). The Kljun *et al.* (2015) model is currently preferred due to its verification over a wider range of atmospheric conditions, and its lower sensitivity to small changes in atmospheric stability.

3.3 Characterisation of conditions in the flux footprint

The resolution of eddy covariance datasets means spatial measurements of sea ice and oceanic conditions within the air-sea gas flux footprint are required to understand the relationship between sea ice and measured CO_2 fluxes and/or inferred gas transfer velocities. Fixed point camera imagery, airborne imagery (e.g. from a helicopter) and satellite remote sensing data have all been used to provide spatial data to characterise sea ice during polar eddy covariance studies (see Table 3). However, not all of the studies identified in this work used spatial data to assess sea-ice conditions (e.g. Miller *et al.*, 2011; Papakyriakou and Miller, 2011; Sørensen *et al.*, 2014; Sievers *et al.*, 2015). Where spatial data has not been used, studies have tended to focus on air-ice-sea interactions and sea-ice has been characterised using vertical sea-ice properties (e.g. ice-depth, ice-temperature, ice-salinity, brine volume) and carbonate chemistry parameters (e.g. total inorganic carbon, total alkalinity). This type of data can only be collected within sea-ice environments where access by foot to collect ice cores is possible (e.g. landfast ice, large ice floes). Ultimately, this approach is limited in its ability to capture spatial heterogeneity at the scales relevant to the eddy covariance flux datasets.

Table 2. Overview of polar eddy covariance air-sea gas flux study sea ice observation methodologies

Study	Sea Ice Observation System	Spatial and Temporal Scale
Semiletov *et al.* (2004)	None.	N/A
Zemmelink *et al.* (2006)	Aerial Photography (visible light) and Electromagnetic soundings	70 km along either side of the floe
Semiletov *et al.* (2007)	None.	N/A
Else *et al.* (2011)	RADARSAT-1 ScanSAR (Synthetic Aperture Radar) narrow beam images.	50 m, as close to each case study as possible
Miller *et al.* (2011)	Ice and snow characteristics from ice cores. No spatial measurements of sea ice.	Discrete sampling, sub-daily
Papakyriakou and Miller (2011)	Sensors deployed in vicinity of EC equipment to measure snow and ice characteristics. No spatial measurements of sea ice.	Discrete sampling, sub-daily
Sørensen et al. (2014)	Ice and snow characteristics from ice cores. No spatial measurements of sea ice.	Discrete sampling, sub-daily
Sievers *et al.* (2015)	Ice and snow characteristics from ice cores. No spatial measurements of sea ice.	Discrete sampling, sub-daily
Butterworth and Miller (2016b)	Two mounted Campbell Scientific CC5MPX digital cameras	Image Footprint - 3000 m^2 (maximum width and length of trapezoid 55 m x 55 m). Photos taken every 1 second.
Prytherch *et al.* (2017)	Satellite Derived Passive Microwave SIC Data from AMSR2 using the Artist sea ice algorithm (ASI 5) (Spreen *et al.*,	6.25 km grid, daily

	2008) interpolated to the flux measurement time.	
Butterworth and Else (2018)	Photos taken with a tower mounted (1) Go Pro Hero 4 and (2) Campbell Scientific CC5MPX digital camera, (3) Satellite Derived Passive Microwave SIC Data from AMSR2 using the Artist sea ice algorithm (ASI 5) (Spreen *et al.*, 2008) (4) Landsat-8 and (5) MODIS images (5) Aerial photographs taken from a helicopter.	(1) unknown, hourly (2) unknown, every 5 minutes (3) 3.125 km grid, daily (4) 30 m, every 8 days dependent on when cloud cover permits (5) 250 m, 1-2 days dependent on when cloud cover permits (6) variable
Prytherch, J. and Yelland, (2021)	Spatial dimensions of lead measured using a hand-held laser range finder (Naturalife PF4)	metres, attempted twice daily.

To characterise ice conditions, Prytherch *et al.* (2017) and Butterworth and Else (2018) used Advanced Microwave Scanning Radiometer 2 (AMSR2) daily SIC derived using the ASI Arctic Radiation and Turbulence Interaction Study (Artist) Sea Ice algorithm (Spreen *et al.*, 2008) at resolutions of 6.25 km and 3.125 km respectively. The Artist sea ice algorithm determines SIC from passive microwave observations, (see = Spreen *et al.* (2008) for further details). Both studies created concurrent time series of daily SIC coincident with measured air-sea gas fluxes, either for the grid-cell matched with the position of the vessel (Prytherch *et al.*, 2017) or with the three grid cells closest to the eddy covariance tower (Butterworth & Else, 2018). Prytherch *et al.* (2017) also linearly interpolated SIC data to the 30-minute resolution flux measurement times.

Butterworth and Miller (2016a) determined SIC using fixed point camera images taken along-track at 1 Hz using digital cameras (CC5MPX; Campbell Scientific) mounted starboard and port on the RV Nathaniel B. Palmer ice-tower. Each image was orthorectified using image coordinates obtained in a laboratory setting input into a geometric transformation script (imwarp.m) from MATLAB's image professing toolbox. To calculate SIC, the rectified images were converted to grayscale and a brightness threshold for ice manually assigned (Hall *et al.* 2002). Manual threshold assignment (not automated) was required due to variability in ice types, light conditions and glare. The percentage of ice pixels was then used to represent ice fraction (e.g. SIC). SIC was calculated in this way for one image every minute and averaged over 10 minutes to create a time-series of SIC concurrent with the gas flux dataset. Each image has a ~3000 m^2 footprint, which represents an area up to ~55 m in front of the vessel. The spatial resolution is thus directly related to the speed of the vessel. The spatial resolution of the extracted SIC data ranges from images with a footprint of ~ 3000 m^2 (i.e. ship's speed is zero) up to an area of horizontal distance of ~ 135,025 m^2 (maximum ship speed of 4 m s^{-1}). These back-of-the-envelope calculations highlight the potential for variability in the spatial resolution of data collected by fixed point camera systems on moving vessels. Bias, driven by natural variations in vessel speed in different ice and oceanic conditions, will therefore need to be characterised in ship-mounted camera derived sea-ice datasets. In the eddy covariance flux studies shown in Table 1, methods to extract SIC from fixed point camera images have been relatively simple (e.g. Hall *et al.*, 2002) and did not result in data with a clearly defined geographical extent. The spatial footprint of each image/image-set is ideally required for eddy covariance studies and should be determined using the field of view of the camera, mount height and viewing angle, camera location (coordinates), camera optics and, if from a moving platform, the speed of the vessel.

Measurement uncertainties associated with different sources of sea-ice data are likely to impact polar air-sea gas flux data interpretation. Uncertainties in passive microwave measurements of SIC can occur when brightness temperature retrievals are affected by atmospheric absorption and emission uncertainties, in particular due to water vapour *(Ivanova et al.*, 2015; Oelke, 1997), wind shear surface roughening effects (Andersen et al., 2006; Oelke, 1997), and smearing effects due to sharp concentration differences within the sensor footprint (Meier, 2005). Passive microwave uncertainties are inherently linked to mixed ice-water environments such as the MIZ, polynyas and the SIZ during autumn-freeze up and spring melt. In addition, wet surfaces (e.g. melt ponds) and thin sea-ice types (< 0.15 m) cannot currently be accurately resolved (Ivanova et al., 2015; Massom, 2009; Meier, 2005). For example, Butterworth and Else (2018) observed that during spring melt season the AMSR2 passive microwave product underestimated SIC by up to 30%, when compared to *in situ* photographs, due to water on the ice surface. Uncertainties associated with SIC data obtained from ship-track or tower-based photos have received limited attention. Fixed point camera image uncertainties include pixel or 'perspective' distortion caused by oblique viewing angles, which causes warping or transformation of the image (Verykokou and Ioannidis, 2018; Zhang and Skjetne, 2018), radial distortion caused by non-rectilinear lenses (Zhang and Skjetne, 2018), and weather and sunlight conditions that influence contrast brightness (Gomez and Purdie, 2016; Kern et al., 2019). There is also potential for SIC differences between ship-based observations and satellite observations due to sampling bias. Ship observations are inherently biased toward low ice concentrations within heterogeneous ice fields because ships avoid thick and deformed sea ice (Kern et al., 2019).

The temporal and spatial resolution of sea-ice data may also impact comparison with eddy covariance flux observations. Eddy covariance datasets have a minimum temporal resolution on the order of 10 to 30 minutes and spatial resolution on the order of 100 m to 2 km (Dong, Yang, Bakker, Kitidis, *et al.*, 2021; Prytherch and Yelland, 2021). Direct comparison of the spatial resolutions of typically available satellite sea-ice data sources and fixed point camera image extent with flux footprints (e.g. as shown in Figure 2) shows major discrepancies in their spatial extent and/or resolution. Mismatched resolutions between the flux data and footprint characterisation data are likely to be important, particularly in highly heterogeneous sea-ice environments. The RADARSAT-1 synthetic aperture radar (SAR) data used by Else *et al.* (2011) has a high spatial resolution (< 50 m) compared to available passive microwave data (3.125 – 25 km) and can be used to determine not only ice concentration, but also ice type (e.g. Else *et al.*, 2011, Park *et al.*, 2019) and ice dynamics (Kozlov *et al.*, 2020; Zhang *et al.*, 2020). Grid-wise data on concentration and ice type extracted from SAR are not yet routinely available but are a promising option for future studies. Optical (visible light spectrum) remote sensing (e.g. Spreen & Kern, 2017) can provide high-spatial resolution imagery useful for many relevant sea ice parameters (e.g. ice concentration, ice type, melt pond fraction) but suffers from even greater temporal constraints due to cloud cover interference. Fixed point camera systems can provide high spatial resolution data, but the specifics vary due to the oblique viewing angle, and its impact on the final resolution of extracted parameters (e.g. SIC) has not been assessed.

Regarding temporal resolution, fixed point camera images can provide sub-daily to sub-hourly SIC as they are not limited by satellite orbit times. SAR data can provide data from which SIC can be extracted typically on a scale of 2-3 days, although this varies geographically and is dependent on the platform orbit and/or constellation. Conversely, passive microwave satellites provide a consistent daily SIC product. How these different resolutions impact results depends on the time-scale of variability of sea-ice conditions within the flux footprint (e.g. how quickly do sea ice conditions in the footprint vary and is this the same for all sea-ice environments?). Ice variability during stationary studies is dependent only on sea-ice processes (e.g. ice melt, ice motion, ice formation), while moving ship-based studies are dependent on ship speed and along-track regional differences in ice conditions (type, distribution). The impact of heterogeneous conditions are also inherently linked to the spatial (size and position) and temporal (variability in time) of the extent of the eddy covariance footprint. The footprint, where the measured gas flux is generated, effectively defines the physical ‘area of interest’ for interpreting the impact of air-ice-sea processes on measured gas fluxes.

Robust interpretations of gas transfer processes in the presence of sea ice require an evaluation of the suitability of flux footprint model input data. The usefulness of sea-ice data is dictated by its spatial and temporal resolutions and the length scale of variability of sea ice compared to the flux footprint extent. Only SIC data derived from passive microwave and fixed point-camera have been used to date to statistically assess sea-ice data and flux footprint analyses. A detailed analysis of the statisitical treatment of percentage sea ice versus eddy covariance flux datasets is needed to identify if results are sensitive to characteristics of the sea ice data used.

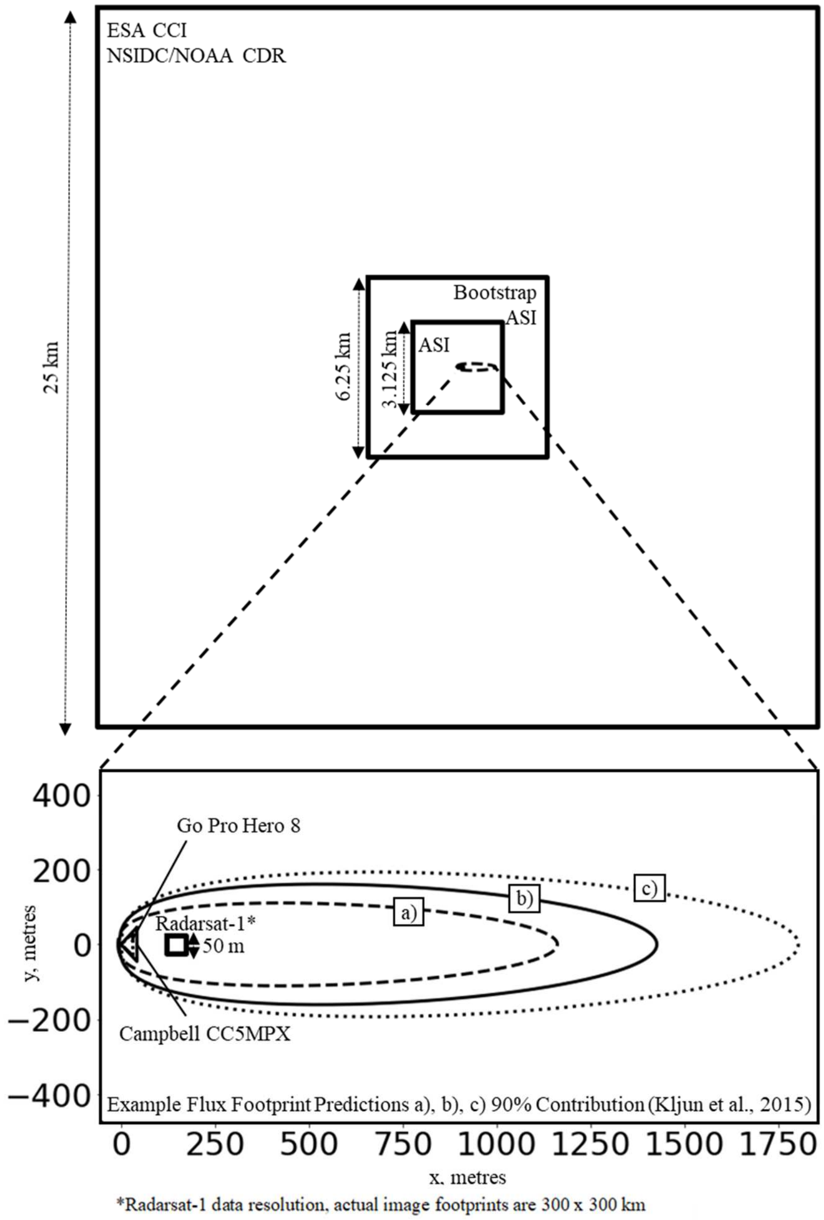

Figure 2. Schematic comparing the footprint of *in situ* camera imaging (Campbell CC5MPX and Go Pro Hero 8, mounted at 12.5 m, angle = 45°) and the spatial resolution of typically available satellite data products (ESA CCI SIC (25 km) NSIDC/NOAA CDR SIC (25 km), AMSR2 ASI V5 SIC (3.125 km, 6.25 km), AMSR2 Bootstrap V5 SIC (6.25 km)) with example flux footprint model estimates (Kljun *et al.* 2015). The flux footprint model (90% contour line) is for a measurement height of 12.5 m, a roughness length (z_0) of 4.1 × 10^2 m (Antarctic pack ice, Weiss *et al.*, 2011): a) frictional velocity (u_*) of 0.2, Obukhov length (L) of -50m and boundary layer height (h) of 2500 m (following the convective scenario 10 in Table 2 of Kljun *et al.*, (2015); b) u_* of 0.3, L of 200 m and h of 310 m (following stable scenario 16, Table 2, Kljun *et al.* (2015); c) represents the footprint for the stable scenario 17 with the same parameters as (b) but a measurement height of 15 m.

353

3.4 Inconsistent air-sea concentration difference measurements and calculations and their impact on gas transfer velocity calculations

Calculating K from eddy covariance datasets requires accurate field measurements of CO_2 on the water-side . (pCO_{2w}))) and the air-side (pCO_{2a}) of the interface (see Eqn. 1)(see Dong et al. (2021a) for an extensive discussion on the accuracy, precision and combined uncertainties associated with these measurements).Thermal and haline effects can significantly influence air-sea gas flux calculations due to their impact on CO_2 solubility, with the dominant effect caused by temperature (Woolf *et al.*, 2016). Typical water sampling techniques (underway systems, niskin bottles) result in sub-surface measurements of pCO_{2w} that need to be corrected to be valid for the interfacial temperature. Vertical gradients occur due to both thermal stratification, which occurs mostly in the summer months due to increased solar radiation, and the 'cool skin effect', whereby the skin temperature (due to heat fluxes) is cooler than the underlying ocean. The impact of the vertical temperature gradients on the pCO_2 difference (ΔpCO_2) is likely to be of the order of 1 to 3 ppm (Woolf, D. personal communication, August 2020). The impact of this on the derived gas transfer will depend on the air-sea pCO_2 difference during each study. For example, the minimum ΔpCO_2 threshold in Prytherch *et al.* (2017) was 40 ppm, which implies a maximum possible error in the resulting K of $\pm$7.5 % if these temperature gradient effects are ignored (i.e. 3/40 = 0.075). This effect should still be considered during the measurement process to minimise its impact, or the issue should be included within the uncertainty budget. Overall, reanalysis of eddy covariance datasets has shown that the impact of near-surface gradients can be anything from small to substantial (see Figure 3 in Holding et al. (2019) and so should be accounted for either wihin the uncertainty budget or quantified during fieldwork.

However, Freshwater inputs into the Arctic Ocean from rivers and sea-ice melt (Yamamato-Kawai *et al.*, 2009) result in widespread vertical stratification. Although salinity has a less significant impact on pCO_{2w} than temperature (Woolf *et al.*, 2019) this haline stratification can result in vertical gradients in pCO_{2w} by suppressing mixing between layers. Field studies in the stratified Arctic found vertical gradients in pCO_{2w} at < 7 m depth (Miller *et al.*, 2019) and < 2 m (Ahmed *et al.* 2020). Ultimately, these field studies suggest large (> 15%) differences in regional (Ahmed *et al.*, 2020) and basin-wide (Miller *et al.*, 2019) flux estimates if sub-surface pCO_{2w} values are used. This effect is also illustrated in Dong et al. (2021b) who used eddy covariance flux measurements to infer that vertical pCO_{2w} gradients, driven predominantly by Arctic sea-ice melt water, could lead to a 6%–17% underestimate of the annual Arctic Ocean CO_2 uptake. Dong et al (2021b) found that if unidentified these gradients in pCO_{2w} can significantly bias the eddy covariance derived K.

In regions with haline stratification differences in pCO_{2w} due to variable measurement depth and water sampling methodology cannot easily be corrected in post-processing, although some authors have tried (e.g Ahmed *et al.* (2020)). Post-processing will be complex and highly uncertain, particularly where multiple processes drive the stratification (Miller *et al.*, 2019). Horizontal variability in pCO_{2w} may also be a concern over the spatial scales commonly captured within a flux footprint. During spring and summer, ice floes that are actively melting can cause plumes of low salinity (and typically low pCO_{2w}) surface water (e.g. Else *et al.*, 2012). Under certain conditions (particularly light winds and low wave state), these plumes could create horizontal gradients on the scale of meters to kilometres that may result in significant pCO_{2w} variability across a flux footprint. Similar issues likely arise during freeze-up, where frazil ice is produced in open water portions of the icescape and then advected horizontally to eventually accrete on the edges of floes (Else *et al.*, 2011). These dynamic processes suggest that a single pCO_{2w} measurement within a flux footprint may not be sufficient to fully characterize the area of interest.

The method of pCO_{2w} measurement method and depth varies in the studies reviewed here (Table 1). For measurements made by the ship's underway system the depths of intake have differed between ~5 m (Else *et al.*, 2011; Butterworth and Miller, 2016a) to ~8 m (Prytherch *et al.*, 2017), as well as rosette samples collected at 5 and 10 m and interpolated (in time and space) to the flux measurement periods (Prytherch et al., 2017). Overall, pCO_{2w} corrections for vertical temperature gradients, the cool skin effect, and differences in water sampling technique are not discussed in any of the studies.

To reduce uncertainties in estimates of K, measurements of pCO_{2w} must be corrected for vertical gradients in temperature (cool skin effect, thermal stratification) in order to represent the surface layer pCO_{2w}. To reduce uncertainty, water samples should be made as close to the surface as possible, or at least verified as being made within the top mixed layer of the ocean. Sampling should ideally be conducted away from large ships to reduce disturbance (Yasunaka *et al.*, 2018), which is challenging when the underway system is the most consistent method of obtaining high temporal and spatial resolution pCO_{2w}. Ideally, several pCO_{2w} measurements would be made across the flux footprint to characterize horizontal gradients. Access to undisturbed pCO_{2w} in surface waters between ice floes is an additional sampling challenge and source of uncertainty. Underway systems are often shut off in brash ice environments to prevent damage to the system and accessing surface waters between floes using other water sampling methodologies (e.g. niskin bottles) is challenging. Ancillary data on the vertical structure (undisturbed by the vessel itself) of the water column (temperature and salinity) and its variability in time and space within the flux footprint should be collected, particularly in physically complex environments (e.g. stratified coastal Arctic waters).

4 Conclusions and recommendations

This work presents an overview and critical review of the findings and methodologies of polar air-sea CO_2 eddy covariance field studies, with a specific focus on gas transfer velocity. There are currently only five studies that present best-practice (closed-path gas analyser, dried or otherwise corrected for humidity bias - see Section 3.1.1) eddy covariance measurements of air-ice-sea CO_2 fluxes and/or air-sea CO_2 fluxes in the presence of sea ice. And three of these studies present estimates of gas transfer velocity in mixed ice-water environments. Clearly conducting eddy covariance field studies in polar regions is challenging due to the harsh and remote environment. But this review highlights that there is a lack of reliable eddy covariance flux measurements over Antarctic multi-year ice (Zemmelink *et al*., 2006) and active polynyas (El*se et al.*, 2011) and no eddy covariance studies of gas transfer velocity during key seasonal processes such as spring-melt season, early ice break up and sea-ice formation. There is a substantial knowledge gap concerning gas exchange in regions of partial to full sea ice coverage, and uncertainties remain greatest in heterogeneous mixed-ice water environments with intermediate SIC. Air-sea gas exchange is uncertain in regions of intermediate ice coverage where observations of the gas transfer velocity are either highly variable or poorly constrained (Fanning and Torres, 2012; Loose et al., 2017; Rutgers Van Der Loeff et al., 2014). Future efforts to understand polar air-sea gas exchange of CO_2 using eddy covariance should be focussed in these environments to improve understanding of whether current sea-ice zone parameterisations of gas transfer are appropriate for use in regional and global air-sea CO_2 flux estimates (research question 3)

Using eddy covariance air-sea CO_2 flux datasets to study the relationship between gas exchange and sea ice requires ancillary data on sea-ice conditions in the air-sea flux footprint. Each of the five highlighted studies in Table 1 has taken a different approach to characterising sea-ice conditions concurrent with measured fluxes. Within this, the impact of using different resolution sea-ice datasets on findings has not been assessed. The spatial and temporal scales of sea-ice data and the flux footprint appear mismatched and the impact of this on flux dataset interpretation remains unexamined.

The ice characterisation in the studies in which the gas transfer velocity is calculated focus largely on SIC. It is likely that the broader impacts of sea ice and ice-water dynamics on gas exchange will need to be considered in order to reconcile theory with field measurements. We recommend that characteristics of the sea ice environment other than SIC are included in future field studies, as supported by Loose *et al.*, (2014) and the findings of Prytherch and Yelland (2021). These could include, but are not limited to: ice type, ice thickness, lead dimensions, ice-water interactions (e.g. ice motion, ice edge stirring), floe size distribution, melt ponds and sea surface roughness.

This review has also highlighted that previous studies used different water sampling techniques at different water depths and without consideration of vertical temperature gradients when calculating the air-sea concentration difference. In addition, any reconciliation of results is further complicated due to incomplete and/or uncalculated uncertainty components that are likely influencing the high variability within any measured fluxes in sea-ice environments.

Overall, without calculated uncertainty components the observed differences in study system and methodology mean the results of historical polar eddy covariance studies of air-sea/air-ice-sea CO_2 fluxes are difficult to objectively compare (research question 1). Key sources of uncertainty in the interpretation of polar eddy covariance flux datasets are identified as: i) the gas analysis technique used, ii) water sampling methodology, iii) corrections for vertical gradients in pCO_{2w}, and iv) the spatial and temporal resolution of data used to characterise the air-sea flux footprint (research question 2).

To reconcile these issues, observations need to be comparable using a standardised methodology along with more complete uncertainty assessments. This should build on the uncertainty assessment made by Dong *et al.*, 2021a in marine environments, which covers uncertainties not discussed in this work (e.g. ship motion, airflow distortion, inlet effects, spatial separation between the anemometer and inlet, sensor calibration and propagated bias). In the open ocean, Dong et al. (2021a) conclude that relative uncertainty in EC CO_2 fluxes is 20-50%, with greater uncertainty when CO_2 fluxes are small. The flux uncertainty can be reduced by averaging for longer (up to 3 hrs), with the required averaging period inversely related to the magnitude of ΔCO_2 The application of a standardised methodology with characterised uncertainties would make it possible to create an inventory of comparable eddy covariance CO_2 flux datasets. Studies can make use of remotely sensed data to characterise conditions within the flux footprint, and the uncertainty of the remote sensing data should be incorporated into the analysis in order to closely examine the process-level controls on air-sea gas exchange in the presence of sea ice. As a starting point for developing a ‘best-practice’ methodology, we recommend the following:

1. Only closed-path gas analysis techniques (either closed-path or cavity ring down gas analysers), with appropriate air-drying and/or water vapour corrections should be used.
2. The length scales of variability of the flux footprint and sea ice compared to the resolution of data characterising the footprint (whether satellite or fixed point-camera) should be characterised. This would need to characterise the full range of environments/ice-water conditions occurring throughout any gas flux data measurement period (as conditions will likely change).
3. Focusing on characterising sea-ice coverage within the modelled flux footprint e.g. build upon the workflow presented in Prytherch and Yelland (2021).
4. For the application of fixed-point cameras, additional work is needed to determine: (i) if the spatial resolution and resultant re-projection of aerial imagery from a fixed-point camera is adequate to characterise conditions within the flux footprint; and (ii) a best practice and consistent method for camera installation and data processing.
5. Water sampling recommendations made in Miller *et al.* (2019) should be followed (i.e. samples collected using a consistent technique and as close to the surface as possible).
6. Air-sea CO_2 concentrations should account for vertical temperature gradients, including the cool skin effect as identified in Watson *et al.* (2020).
7. Collection of ancillary data on $p\mathrm{CO}_{2w}$ gradients and water column structure, particularly away from the vessel if an underway system is being used, is recommended to aid interpretation of results

Acknowledgments

This work is supported by a NERC PhD studentship (NE/L002434/1) as part of the GW4+ Doctoral Training Program. The contribution of T. Bell was supported by the NERC funded ORCHESTRA (NE/N018095/1) and PICCOLO (NE/P021409/1) projects. We also thank J.Prytherch for a constructive review of the manuscript prior to publication.

References

Ahmed, M.M.M., Else, B.G.T., Capelle, D., Miller, L.A., Papakyriakou, T., 2020. Underestimation of surface p CO2 and air-sea CO2 fluxes due to freshwater stratification in an Arctic shelf sea, Hudson Bay . Elem. Sci. Anthr. 8. https://doi.org/10.1525/elementa.084

Andersen, S., Tonboe, R., Kern, S., Schyberg, H., 2006. Improved retrieval of sea ice total concentration from spaceborne passive microwave observations using numerical weather prediction model fields: An intercomparison of nine algorithms. Remote Sens. Environ. 104, 374–392. https://doi.org/10.1016/j.rse.2006.05.013

Andreas, E.L., Horst, T.W., Grachev, A.A., Persson, P.O.G., Fairall, C.W., Guest, P.S., Jordan, R.E., 2010. Parametrizing turbulent exchange over summer sea ice and the marginal ice zone. Q. J. R. Meteorol. Soc. 136, 927–943. https://doi.org/10.1002/qj.618

Arrigo, K.R., Van Dijken, G.L., 2007. Interannual variation in air-sea CO2 flux in the Ross Sea, Antarctica: A model analysis. J. Geophys. Res. Ocean. 112, C03020. https://doi.org/10.1029/2006JC003492

Banko-Kubis, H.M., Wurl, O., Mustaffa, N.I.H., Ribas-Ribas, M., 2019. Gas transfer velocities in Norwegian fjords and the adjacent North Atlantic waters. Oceanologia 61, 460–470. https://doi.org/10.1016/j.oceano.2019.04.002

Bates, N.R., Mathis, J.T., 2009. The Arctic Ocean marine carbon cycle: Evaluation of air-sea CO2 exchanges, ocean acidification impacts and potential feedbacks. Biogeosciences 6, 2433–2459. https://doi.org/10.5194/bg-6-2433-2009

Bell, T.G., De Bruyn, W., Marandino, C.A., Miller, S.D., Law, C.S., Smith, M.J., Saltzman, E.S., 2015. Dimethylsulfide gas transfer coefficients from algal blooms in the Southern Ocean 15, 1783–1794. https://doi.org/10.5194/acp-15-1783-2015

Bell, T.G., Landwehr, S., Miller, S.D., De Bruyn, W.J., Callaghan, A.H., Scanlon, B., Ward, B., Yang, M., Saltzman, E.S., 2017. Estimation of bubble-mediated air-sea gas exchange from concurrent DMS and CO2 transfer velocities at intermediate-high wind speeds. Atmos. Chem. Phys. 17, 9019–9033. https://doi.org/10.5194/acp-17-9019-2017

Bigdeli, A., Hara, T., Loose, B., Nguyen, A.T., 2018. Wave Attenuation and Gas Exchange Velocity in Marginal Sea Ice Zone. J. Geophys. Res. Ocean. 123, 2293–2304. https://doi.org/10.1002/2017JC013380

Blomquist, B.W., Brumer, S.E., Fairall, C.W., Huebert, B.J., Zappa, C.J., Brooks, I.M., Yang, M., Bariteau, L., Prytherch, J., Hare, J.E., Czerski, H., Matei, A., Pascal, R.W., 2017. Wind Speed and Sea State Dependencies of Air-Sea Gas Transfer: Results From the High Wind Speed Gas Exchange Study (HiWinGS). J. Geophys. Res. Ocean. 122, 8034–8062. https://doi.org/10.1002/2017JC013181

Blomquist, B.W., Huebert, B.J., Fairall, C.W., Bariteau, L., Edson, J.B., Hare, J.E., McGillis, W.R., 2014. Advances in Air-Sea CO2 Flux Measurement by Eddy Correlation. Boundary-Layer Meteorol. 152, 245–276. https://doi.org/10.1007/s10546-014-9926-2

Butterworth, B.J., Else, B.G.T., 2018. Dried , closed-path eddy covariance method for measuring carbon dioxide flux over sea ice. Atmos. Meas. Tech. 6075–6090. https://doi.org/10.5194/amt-11-6075-2018

Butterworth, B.J., Miller, S.D., 2016a. Automated underway eddy covariance system for air-sea momentum, heat, and CO2 fluxes in the Southern Ocean. J. Atmos. Ocean. Technol. 33, 635–652. https://doi.org/10.1175/JTECH-D-15-0156.1

Butterworth, B.J., Miller, S.D., 2016b. Air-sea exchange of carbon dioxide in the Southern Ocean and Antarctic marginal ice zone. Geophys. Res. Lett. 43, 7223–7230. https://doi.org/10.1002/2016GL069581

Caldeira, K., Duffy, P.B., 2000. The role of the southern ocean in uptake and storage of anthropogenic carbon dioxide. Science (80-.). 287, 620–622. https://doi.org/10.1126/science.287.5453.620

Clarke, J.S., Achterberg, E.P., Connelly, D.P., Schuster, U., Mowlem, M., 2017. Developments in marine pCO2 measurement technology; towards sustained in situ observations. TrAC - Trends Anal. Chem. https://doi.org/10.1016/j.trac.2016.12.008

Deike, L., Melville, W.K., 2018. Gas Transfer by Breaking Waves. Geophys. Res. Lett. 45, 10,482-10,492. https://doi.org/10.1029/2018GL078758

Devries, T., 2014. The oceanic anthropogenic CO2 sink: Storage, air-sea fluxes, and transports over the industrial era. Global Biogeochem. Cycles 28, 631–647. https://doi.org/10.1002/2013GB004739

Dong, Y., Yang, M., Bakker, D., Kitidis, V., Bell, T., 2021a. Uncertainties in eddy covariance air-sea CO_2 flux measurements and implications for gas transfer velocity parameterisations. Atmos. Chem. Phys. 1–43. https://doi.org/10.5194/acp-2021-120

Dong, Y., Yang, M., Bakker, D.C.E., Liss, P.S., Kitidis, V., Brown, I., Chierici, M., Fransson, A., Bell, T.G., 2021b. Near-surface Stratification Due to Ice Melt Biases Arctic Air-Sea CO 2 Flux Estimates . Geophys. Res. Lett. 1–10. https://doi.org/10.1029/2021gl095266

Else, B.G.T., Papakyriakou, T.N., Galley, R.J., Drennan, W.M., Miller, L.A., Thomas, H., 2011.

Wintertime CO2 fluxes in an Arctic polynya using eddy covariance: Evidence for enhanced air-sea gas transfer during ice formation. J. Geophys. Res. Ocean. 116, 0–03. https://doi.org/10.1029/2010JC006760

Fanning, K.A., Torres, L.M., 2012. 222 Rn and 226 Ra: indicators of sea-ice effects on air-sea gas exchange . Polar Res. 10, 51–58. https://doi.org/10.3402/polar.v10i1.6727

Friedlingstein, P., O'Sullivan, M., Jones, M.W., Andrew, R.M., Hauck, J., Olsen, A., Peters, G.P., Peters, W., Pongratz, J., Sitch, S., Le Quéré, C., Canadell, J.G., Ciais, P., Jackson, R.B., Alin, S., Aragão, L.E.O.C., Arneth, A., Arora, V., Bates, N.R., Becker, M., Benoit-Cattin, A., Bittig, H.C., Bopp, L., Bultan, S., Chandra, N., Chevallier, F., Chini, L.P., Evans, W., Florentie, L., Forster, P.M., Gasser, T., Gehlen, M., Gilfillan, D., Gkritzalis, T., Gregor, L., Gruber, N., Harris, I., Hartung, K., Haverd, V., Houghton, R.A., Ilyina, T., Jain, A.K., Joetzjer, E., Kadono, K., Kato, E., Kitidis, V., Korsbakken, J.I., Landschützer, P., Lefèvre, N., Lenton, A., Lienert, S., Liu, Z., Lombardozzi, D., Marland, G., Metzl, N., Munro, D.R., Nabel, J.E.M.S., Nakaoka, S.I., Niwa, Y., O'Brien, K., Ono, T., Palmer, P.I., Pierrot, D., Poulter, B., Resplandy, L., Robertson, E., Rödenbeck, C., Schwinger, J., Séférian, R., Skjelvan, I., Smith, A.J.P., Sutton, A.J., Tanhua, T., Tans, P.P., Tian, H., Tilbrook, B., Van Der Werf, G., Vuichard, N., Walker, A.P., Wanninkhof, R., Watson, A.J., Willis, D., Wiltshire, A.J., Yuan, W., Yue, X., Zaehle, S., 2020. Global Carbon Budget 2020. Earth Syst. Sci. Data 12, 3269–3340. https://doi.org/10.5194/essd-12-3269-2020

Gao, K., Helbling, E.W., Häder, D.P., Hutchins, D.A., 2012. Responses of marine primary producers to interactions between ocean acidification, solar radiation, and warming. Mar. Ecol. Prog. Ser. 470, 167–189. https://doi.org/10.3354/meps10043

Gattuso, J.P., Magnan, A., Billé, R., Cheung, W.W.L., Howes, E.L., Joos, F., Allemand, D., Bopp, L., Cooley, S.R., Eakin, C.M., Hoegh-Guldberg, O., Kelly, R.P., Pörtner, H.O., Rogers, A.D., Baxter, J.M., Laffoley, D., Osborn, D., Rankovic, A., Rochette, J., Sumaila, U.R., Treyer, S., Turley, C., 2015. Contrasting futures for ocean and society from different anthropogenic CO2 emissions scenarios. Science (80-.). https://doi.org/10.1126/science.aac4722

Geilfus, N.X., Tison, J.L., Ackley, S.F., Galley, R.J., Rysgaard, S., Miller, L.A., Delille, B., 2014. Sea ice pCO2 dynamics and air-ice CO2 fluxes during the sea ice mass balance in the Antarctic (SIMBA) experiment – Bellingshausen sea, Antarctica. Cryosphere 8, 2395–2407. https://doi.org/10.5194/tc-8-2395-2014

Gomez, C., Purdie, H., 2016. UAV- based Photogrammetry and Geocomputing for Hazards and Disaster Risk Monitoring – A Review. Geoenvironmental Disasters. https://doi.org/10.1186/s40677-016-0060-y

Guest, P.S., Davidson, K.L., 1991. The aerodynamic roughness of different types of sea ice. J. Geophys. Res. 96, 4709–4721. https://doi.org/10.1029/90JC02261

Hill, T., Chocholek, M., Clement, R., 2017. The case for increasing the statistical power of eddy covariance ecosystem studies: why, where and how? Glob. Chang. Biol. 23, 2154–2165. https://doi.org/10.1111/gcb.13547

Ho, D.T., Wanninkhof, R., Schlosser, P., Ullman, D.S., Hebert, D., Sullivan, K.F., 2011. Toward a universal relationship between wind speed and gas exchange: Gas transfer velocities measured with 3He/SF6 during the Southern Ocean Gas Exchange Experiment. J. Geophys. Res. Ocean. 116. https://doi.org/10.1029/2010JC006854

Holding, T., Ashton, I.G., Shutler, J.D., Land, P.E., Nightingale, P.D., Rees, A.P., Brown, I., Piolle, J.F., Kock, A., Bange, H.W., Woolf, D.K., Goddijn-Murphy, L., Pereira, R., Paul, F., Girard-Ardhuin, F., Chapron, B., Rehder, G., Ardhuin, F., Donlon, C.J., 2019. The fluxengine air-sea gas flux toolbox: Simplified interface and extensions for in situ analyses and multiple sparingly soluble gases. Ocean Sci. 15, 1707–1728. https://doi.org/10.5194/os-15-1707-2019

Hsieh, C.I., Katul, G., Chi, T.W., 2000. An approximate analytical model for footprint estimation of scalar fluxes in thermally stratified atmospheric flows. Adv. Water Resour. 23, 765–772. https://doi.org/10.1016/S0309-1708(99)00042-1

Ivanova, N., Pedersen, L.T., Tonboe, R.T., Kern, S., Heygster, G., Lavergne, T., Sørensen, A., Saldo, R., Dybkjær, G., Brucker, L., Shokr, M., 2015. Inter-comparison and evaluation of sea ice algorithms: Towards further identification of challenges and optimal approach using passive microwave observations. Cryosphere 9, 1797–1817. https://doi.org/10.5194/tc-9-1797-2015

Jentzsch, K., Boike, J., Foken, T., 2021. Importance of the WPL correction for the measurement of small CO2 fluxes. Atmos. Meas. Tech. Discuss. 1–10. https://doi.org/10.5194/amt-2021-249

Kern, S., Lavergne, T., Notz, D., Toudal Pedersen, L., Tage Tonboe, R., Saldo, R., Macdonald Sørensen, A., 2019. Satellite passive microwave sea-ice concentration data set intercomparison: Closed ice and ship-based observations. Cryosphere 13, 3261–3307. https://doi.org/10.5194/tc-13-3261-2019

Kljun, N., Calanca, P., Rotach, M.W., Schmid, H.P., 2015. A simple two-dimensional parameterisation for Flux Footprint Prediction (FFP). Geosci. Model Dev. 8, 3695–3713. https://doi.org/10.5194/gmd-8-3695-2015

Kohout, A.L., Meylan, M.H., 2008. An elastic plate model for wave attenuation and ice floe breaking in the marginal ice zone. J. Geophys. Res. 113, C09016. https://doi.org/10.1029/2007JC004434

Kohsiek, W., 2000. Water Vapor Cross-Sensitivity of Open Path H_2O/CO_2 Sensors. J. Atmos. Ocean. Technol. 17, 299–311. https://doi.org/10.1175/1520-0426(2000)017<0299:WVCSOO>2.0.CO;2

Kozlov, I.E., Plotnikov, E. V., Manucharyan, G.E., 2020. Brief Communication: Mesoscale and submesoscale dynamics in the marginal ice zone from sequential synthetic aperture radar observations. Cryosphere 14, 2941–2947. https://doi.org/10.5194/tc-14-2941-2020

Kwok, R., Rothrock, D.A., 2009. Decline in Arctic sea ice thickness from submarine and ICESat records: 1958-2008. Geophys. Res. Lett. 36, n/a-n/a. https://doi.org/10.1029/2009GL039035

Kwok, R., Untersteiner, N., 2011. The thinning of Arctic sea ice. Phys. Today 64, 36–41. https://doi.org/10.1063/1.3580491

Landwehr, S., Miller, S.D., Smith, M.J., Bell, T.G., Saltzman, E.S., Ward, B., 2018. Using eddy covariance to measure the dependence of air-sea CO2 exchange rate on friction velocity. Atmos. Chem. Phys. 18, 4297–4315. https://doi.org/10.5194/acp-18-4297-2018

Landwehr, S., Miller, S.D., Smith, M.J., Saltzman, E.S., Ward, B., 2014. Analysis of the PKT correction for direct CO2 flux measurements over the ocean. Atmos. Chem. Phys. 14, 3361–3372. https://doi.org/10.5194/acp-14-3361-2014

Landwehr, S., O'Sullivan, N., Ward, B., 2015. Direct flux measurements from mobile platforms at sea: Motion and airflow distortion corrections revisited. J. Atmos. Ocean. Technol. 32, 1163–1178. https://doi.org/10.1175/JTECH-D-14-00137.1

Liss, P.S., Slater, P.G., 1974. Flux of gases across the Air-Sea interface. Nature 247, 181–184.

https://doi.org/10.1038/247181a0
Loose, B., Kelly, R.P., Bigdeli, A., Williams, W., Krishfield, R., Rutgers van der Loeff, M., Moran, S.B., 2017. How well does wind speed predict air-sea gas transfer in the sea ice zone? A synthesis of radon deficit profiles in the upper water column of the Arctic Ocean. J. Geophys. Res. Ocean. 122, 3696–3714. https://doi.org/10.1002/2016JC012460
Loose, B., McGillis, W.R., Perovich, D., Zappa, C.J., Schlosser, P., 2014. A parameter model of gas exchange for the seasonal sea ice zone. Ocean Sci. 10, 17–28. https://doi.org/10.5194/os-10-17-2014
Lovely, A., Loose, B., Schlosser, P., McGillis, W., Zappa, C., Perovich, D., Brown, S., Morell, T., Hsueh, D., Friedrich, R., 2015. The Gas Transfer through Polar Sea ice experiment: Insights into the rates and pathways that determine geochemical fluxes. J. Geophys. Res. Ocean. 120, 8177–8194. https://doi.org/10.1002/2014JC010607
Lubin, D., Wittenmyer, R.A., Bromwich, D.H., Marshall, G.J., 2008. Antarctic Peninsula mesoscale cyclone variability and climatic impacts influenced by the SAM. Geophys. Res. Lett. 35, L02808. https://doi.org/10.1029/2007GL032170
MacGilchrist, G.A., Naveira Garabato, A.C., Tsubouchi, T., Bacon, S., Torres-Valdés, S., Azetsu-Scott, K., 2014. The Arctic Ocean carbon sink. Deep. Res. Part I Oceanogr. Res. Pap. 86, 39–55. https://doi.org/10.1016/j.dsr.2014.01.002
Massom, R.A., 2009. Principal uses of remote sensing in a sea ice field research. F. Tech. Sea Ice Res. 405–466.
Massom, R.A., Stammerjohn, S.E., 2010. Antarctic sea ice change and variability - Physical and ecological implications. Polar Sci. 4, 149–186. https://doi.org/10.1016/j.polar.2010.05.001
McPhee, M.G., Martinson, D.G., 1994. Turbulent mixing under drifting pack ice in the Weddell Sea. Science (80-.). 263, 218–221. https://doi.org/10.1126/science.263.5144.218
Meier, W.N., 2005. Comparison of passive microwave ice concentration algorithm retrievals with AVHRR imagery in arctic peripheral seas. IEEE Trans. Geosci. Remote Sens. 43, 1324–1337. https://doi.org/10.1109/TGRS.2005.846151
Meier, W.N., Stroeve, J., Fetterer, F., 2007. Whither Arctic sea ice? A clear signal of decline regionally, seasonally and extending beyond the satellite record, in: Annals of Glaciology. pp. 428–434. https://doi.org/10.3189/172756407782871170
Mikaloff Fletcher, S.E., Gruber, N., Jacobson, A.R., Doney, S.C., Dutkiewicz, S., Gerber, M., Follows, M., Joos, F., Lindsay, K., Menemenlis, D., Mouchet, A., Müller, S.A., Sarmiento, J.L., 2006. Inverse estimates of anthropogenic CO2 uptake, transport, and storage by the ocean. Global Biogeochem. Cycles 20, 1–16. https://doi.org/10.1029/2005GB002530
Miller, L.A., Burgers, T.M., Burt, W.J., Granskog, M.A., Papakyriakou, T.N., 2019. Air-Sea CO 2 Flux Estimates in Stratified Arctic Coastal Waters: How Wrong Can We Be? Geophys. Res. Lett. 46, 235–243. https://doi.org/10.1029/2018GL080099
Miller, L.A., Carnat, G., Else, B.G.T., Sutherland, N., Papakyriakou, T.N., 2011a. Carbonate system evolution at the Arctic Ocean surface during autumn freeze-up. J. Geophys. Res. Ocean. 116. https://doi.org/10.1029/2011JC007143
Miller, L.A., Papakyriakou, T.N., Collins, R Eric, Deming, Jody W, Ehn, Jens K, Macdonald, Robie W, Mucci, Alfonso, Owens, Owen, Raudsepp, Mati, Sutherland, Nes, Papakyriakou, N., Collins, R E, Deming, J W, Ehn, J K, Macdonald, R W, Mucci, A, Owens, O, Raudsepp, M, Sutherland, N, 2011b. Carbon dynamics in sea ice: A winter flux time series. J. Geophys. Res 116, 2028. https://doi.org/10.1029/2009JC006058
Miller, S., Marandino, C., Saltzman, E.S., 2010. Ship-based measurement of air-sea CO 2

exchange by eddy covariance. J. Geophys. Res. 115, D02304. https://doi.org/10.1029/2009JD012193

Miller, S.D., Marandino, C.A., DeBruyn, W.J., Saltzman, E.S., 2009. Eddy correlation carbon dioxide and dimethlysulfide air-sea gas exchange in the North Atlantic. Geophys. Res. Lett 36, L15816.

Morison, J.H., McPhee, M.G., Curtin, T.B., Paulson, C.A., 1992. The Oceanography of Winter Leads. J. Geophys. Res. 97, 11199–11218. https://doi.org/10.1029/92jc00684

Oelke, C., 1997. Atmospheric signatures in sea-ice concentration estimates from passive microwaves: Modelled and observed. Int. J. Remote Sens. 18, 1113–1136. https://doi.org/10.1080/014311697218601

Papakyriakou, T., Miller, L.A., 2011. Springtime CO2 exchange over seasonal sea ice in the Canadian Arctic Archipelago. Ann. Glaciol. 52, 215–224. https://doi.org/10.3189/172756411795931534

Park, J.-W., Korosov, A., Babiker, M., Kim, H.-C., 2019. Automated Sea Ice Classification Using Sentinel-1 Imagery, in: IGARSS 2019 - 2019 IEEE International Geoscience and Remote Sensing Symposium. IEEE, pp. 4008–4011. https://doi.org/10.1109/IGARSS.2019.8898731

Parkinson, C.L., 2019. A 40-y record reveals gradual Antarctic sea ice increases followed by decreases at rates far exceeding the rates seen in the Arctic. Proc. Natl. Acad. Sci. U. S. A. 116, 14414–14423. https://doi.org/10.1073/pnas.1906556116

Pereira, R., Ashton, I., Sabbaghzadeh, B., Shutler, J.D., Upstill-Goddard, R.C., 2018. Reduced air-sea CO2 exchange in the Atlantic Ocean due to biological surfactants. Nat. Geosci. 11, 492–496. https://doi.org/10.1038/s41561-018-0136-2

Prytherch, J., Brooks, I.M., Crill, P.M., Thornton, B.F., Salisbury, D.J., Tjernström, M., Anderson, L.G., Geibel, M.C., Humborg, C., 2017. Direct determination of the air-sea CO2 gas transfer velocity in Arctic sea ice regions. Geophys. Res. Lett. 44, 3770–3778. https://doi.org/10.1002/2017GL073593

Prytherch, J., Yelland, M.J., 2021. Wind, Convection and Fetch Dependence of Gas Transfer Velocity in an Arctic Sea-Ice Lead Determined From Eddy Covariance CO2 Flux Measurements. Global Biogeochem. Cycles 35. https://doi.org/10.1029/2020GB006633

Rutgers Van Der Loeff, M.M., Cassar, N., Nicolaus, M., Rabe, B., Stimac, I., 2014. The influence of sea ice cover on air-sea gas exchange estimated with radon-222 profiles. J. Geophys. Res. Ocean. 119, 2735–2751. https://doi.org/10.1002/2013JC009321

Semiletov, I., Makshtas, A., Akasofu, S.I., Andreas, E.L., 2004. Atmospheric CO2 balance: The role of Arctic sea ice. Geophys. Res. Lett. 31, n/a-n/a. https://doi.org/10.1029/2003gl017996

Semiletov, I., Pipko, I.I., Repina, I., Shakhova, N.E., 2007. Carbonate chemistry dynamics and carbon dioxide fluxes across the atmosphere-ice-water interfaces in the Arctic Ocean: Pacific sector of the Arctic. J. Mar. Syst. 66, 204–226. https://doi.org/10.1016/j.jmarsys.2006.05.012

Serreze, M.C., Barry, R.G., 2011. Processes and impacts of Arctic amplification: A research synthesis. Glob. Planet. Change 77, 85–96. https://doi.org/10.1016/j.gloplacha.2011.03.004

Serreze, M.C., Stroeve, J., 2015. Arctic sea ice trends, variability and implications for seasonal ice forecasting. Philos. Trans. R. Soc. A Math. Phys. Eng. Sci. 373. https://doi.org/10.1098/rsta.2014.0159

Shutler, J.D., Land, P.E., Piolle, J.F., Woolf, D.K., Goddijn-Murphy, L., Paul, F., Girard-Ardhuin, F., Chapron, B., Donlon, C.J., 2016. FluxEngine: A flexible processing system for calculating atmosphere-ocean carbon dioxide gas fluxes and climatologies. J. Atmos. Ocean. Technol. 33, 741–756. https://doi.org/10.1175/JTECH-D-14-00204.1

Shutler, J.D., Wanninkhof, R., Nightingale, P.D., Woolf, D.K., Bakker, D.C., Watson, A., Ashton, I., Holding, T., Chapron, B., Quilfen, Y., Fairall, C., Schuster, U., Nakajima, M., Donlon, C.J., 2020. Satellites will address critical science priorities for quantifying ocean carbon. Front. Ecol. Environ. https://doi.org/10.1002/fee.2129

Sievers, J., Sørensen, L.L., Papakyriakou, T., Else, B., Sejr, M.K., Haubjerg Søgaard, D., Barber, D., Rysgaard, S., 2015. Winter observations of CO₂ exchange between sea ice and the atmosphere in a coastal fjord environment. Cryosph. 9, 1701–1713. https://doi.org/10.5194/tc-9-1701-2015

Smeets, C.J.P.P., Broeke, M.R., 2008. Temporal and spatial variations of the aerodynamic roughness length in the ablation zone of the greenland ice sheet. Boundary-Layer Meteorol. 128, 315–338. https://doi.org/10.1007/s10546-008-9291-0

Sørensen, L.L., Jensen, B., Glud, R.N., McGinnis, D.F., Sejr, M.K., Sievers, J., Søgaard, D.H., Tison, J.L., Rysgaard, S., 2014. Parameterization of atmosphere-surface exchange of CO2 over sea ice. Cryosphere 8, 853–866. https://doi.org/10.5194/tc-8-853-2014

Stammerjohn, S.E., Martinson, D.G., Smith, R.C., Yuan, X., Rind, D., 2008. Trends in Antarctic annual sea ice retreat and advance and their relation to El Niño–Southern Oscillation and Southern Annular Mode variability. J. Geophys. Res. 113. https://doi.org/10.1029/2007jc004269

Stephens, B.B., Keeling, R.F., 2000. The influence of antarctic sea ice on glacial-interglacial CO2 variations. Nature 404, 171–174. https://doi.org/10.1038/35004556

Stroeve, J.C., Kattsov, V., Barrett, A., Serreze, M., Pavlova, T., Holland, M., Meier, W.N., 2012. Trends in Arctic sea ice extent from CMIP5, CMIP3 and observations. Geophys. Res. Lett. 39, n/a-n/a. https://doi.org/10.1029/2012GL052676

Strong, C., Rigor, I.G., 2013. Arctic marginal ice zone trending wider in summer and narrower in winter. Geophys. Res. Lett. 40, 4864–4868. https://doi.org/10.1002/grl.50928

Takahashi, T., Sutherland, S.C., Wanninkhof, R., Sweeney, C., Feely, R.A., Chipman, D.W., Hales, B., Friederich, G., Chavez, F., Sabine, C., Watson, A., Bakker, D.C.E., Schuster, U., Metzl, N., Yoshikawa-Inoue, H., Ishii, M., Midorikawa, T., Nojiri, Y., Körtzinger, A., Steinhoff, T., Hoppema, M., Olafsson, J., Arnarson, T.S., Tilbrook, B., Johannessen, T., Olsen, A., Bellerby, R., Wong, C.S., Delille, B., Bates, N.R., de Baar, H.J.W., 2009. Climatological mean and decadal change in surface ocean pCO2, and net sea-air CO2 flux over the global oceans. Deep. Res. Part II Top. Stud. Oceanogr. 56, 554–577. https://doi.org/10.1016/j.dsr2.2008.12.009

Verykokou, S., Ioannidis, C., 2018. Oblique aerial images: a review focusing on georeferencing procedures. Int. J. Remote Sens. https://doi.org/10.1080/01431161.2018.1444294

Wanninkhof, R., 2014. Relationship between wind speed and gas exchange over the ocean revisited. Limnol. Oceanogr. Methods 12, 351–362. https://doi.org/10.4319/lom.2014.12.351

Wanninkhof, R., Asher, W.E., Ho, D.T., Sweeney, C., McGillis, W.R., 2009. Advances in Quantifying Air-Sea Gas Exchange and Environmental Forcing. Ann. Rev. Mar. Sci. 1, 213–244. https://doi.org/10.1146/annurev.marine.010908.163742

Watson, A.J., Schuster, U., Shutler, J.D., Holding, T., Ashton, I.G.C., Landschützer, P., Woolf, D.K., Goddijn-Murphy, L., 2020. Revised estimates of ocean-atmosphere CO2 flux are consistent with ocean carbon inventory. Nat. Commun. 11, 1–6. https://doi.org/10.1038/s41467-020-18203-3

Webb, E.K., Pearman, G.I., Leuning, R., 1980. Correction of flux measurements for density effects due to heat and water vapour transfer. Q. J. R. Meteorol. Soc. 106, 85–100. https://doi.org/10.1002/qj.49710644707

Weiss, A.I., King, J., Lachlan-Cope, T., Ladkin, R., 2011. On the effective aerodynamic and scalar roughness length of Weddell Sea ice. J. Geophys. Res. 116, D19119. https://doi.org/10.1029/2011JD015949

Woolf, D.K., Land, P.E., Shutler, J.D., Goddijn-Murphy, L.M., Donlon, C.J., 2016. On the calculation of air-sea fluxes of CO 2 in the presence of temperature and salinity gradients. J. Geophys. Res. Ocean. 121, 1229–1248. https://doi.org/10.1002/2015JC011427

Woolf, D.K., Shutler, J.D., Goddijn-Murphy, L., Watson, A.J., Chapron, B., Nightingale, P.D., Donlon, C.J., Piskozub, J., Yelland, M.J., Ashton, I., Holding, T., Schuster, U., Girard-Ardhuin, F., Grouazel, A., Piolle, J. -F., Warren, M., Wrobel-Niedzwiecka, I., Land, P.E., Torres, R., Prytherch, J., Moat, B., Hanafin, J., Ardhuin, F., Paul, F., 2019. Key Uncertainties in the Recent Air-Sea Flux of CO 2. Global Biogeochem. Cycles 33, 1548–1563. https://doi.org/10.1029/2018GB006041

Yang, M., Prytherch, J., Kozlova, E., Yelland, M.J., Parenkat Mony, D., Bell, T.G., 2016. Comparison of two closed-path cavity-based spectrometers for measuring air-water CO2 and CH4 fluxes by eddy covariance. Atmos. Meas. Tech. 9, 5509–5522. https://doi.org/10.5194/amt-9-5509-2016

Yang, M., Smyth, T.J., Kitidis, V., Brown, I.J., Wohl, C., Yelland, M.J., Bell, T.G., 2021. Natural variability in air–sea gas transfer efficiency of CO_2 Sci. Rep. 11, 1–9. https://doi.org/10.1038/s41598-021-92947-w

Yasunaka, S., Murata, A., Watanabe, E., Chierici, M., Fransson, A., van Heuven, S., Hoppema, M., Ishii, M., Johannessen, T., Kosugi, N., Lauvset, S.K., Mathis, J.T., Nishino, S., Omar, A.M., Olsen, A., Sasano, D., Takahashi, T., Wanninkhof, R., Omar, A.M., Lauvset, S.K., Watanabe, E., Kosugi, N., Olsen, A., Mathis, J.T., van Heuven, S., Ishii, M., Sasano, D., Murata, A., Fransson, A., Chierici, M., Nishino, S., Yasunaka, S., Takahashi, T., Hoppema, M., Johannessen, T., 2016. Mapping of the air–sea CO2 flux in the Arctic Ocean and its adjacent seas: Basin-wide distribution and seasonal to interannual variability. Polar Sci. 10, 323–334. https://doi.org/10.1016/j.polar.2016.03.006

Yasunaka, S., Siswanto, E., Olsen, A., Hoppema, M., Watanabe, E., Fransson, A., Chierici, M., Murata, A., Lauvset, S.K., Wanninkhof, R., Takahashi, T., Kosugi, N., Omar, A.M., Van Heuven, S., Mathis, J.T., 2018. Arctic Ocean CO 2 uptake: an improved multiyear estimate of the air-sea CO 2 flux incorporating chlorophyll a concentrations. Biogeosciences 15, 1643–1661. https://doi.org/10.5194/bg-15-1643-2018

Zavarsky, A., Goddijn-Murphy, L., Steinhoff, T., Marandino, C.A., 2018. Bubble-Mediated Gas Transfer and Gas Transfer Suppression of DMS and CO_2 J. Geophys. Res. Atmos. 123, 6624–6647. https://doi.org/10.1029/2017JD028071

Zemmelink, H.J., Delille, B., Tison, J.L., Hintsa, E.J., Houghton, L., Dacey, J.W.H., 2006. CO2 deposition over the multi-year ice of the western Weddell Sea. Geophys. Res. Lett. 33, L13606. https://doi.org/10.1029/2006GL026320

Zhang, Q., Skjetne, R., 2018. Sea Ice Image Processing with MATLAB®. CRC Press.

Zhang, X., Zhu, Y., Zhang, J., Meng, J., Li, Xiaona, Li, Xingxing, 2020. An Algorithm for Sea Ice Drift Retrieval Based on Trend of Ice Drift Constraints from Sentinel-1 SAR Data. J.

Coast. Res. 102, 113–126. https://doi.org/10.2112/SI102-015.1

Progress in Oceanography

Supporting Information for

Sea ice and air-sea CO2 exchange – a critical review of polar eddy covariance studies

Jennifer Watts[1]*, Thomas G. Bell[2], Karen Anderson[3], Brian J. Butterworth[4], Scott Miller[5], Brent Else[6], Jamie Shutler[1]

[1] College of Life and Environmental Sciences, University of Exeter, Penryn, Cornwall, UK.

[1]Plymouth Marine Laboratory, Plymouth, Devon, UK.

[3]Environment and Sustainability Institute, University of Exeter, Penryn, Cornwall.

[4]University of Wisconsin-Madison, Madison, Wisconsin, USA.

[5]Atmospheric Sciences Research Centre, University of Albany (State University of New York), USA.

[6]Department of Geography, University of Calgary, Canada.

*Corresponding author: Jennifer Watts (j.h.watts@exeter.ac.uk)

Contents of this file

Introduction

This supporting information presents a detailed description of the study system, experimental set-up and conclusions of twelve polar eddy covariance studies identified via a literature review.

Table S1. Synthesis of polar EC air-sea CO_2 gas flux studies study systems, equipment, data process and footprint characterisation.

Study Overview					Eddy Covariance Equipment			Data Processing			Sea Ice Characterisation	
Study	Location	Description	Dates	Platform	Gas Analysers	Air-Drying	Wind	Corrections	Gas Transfer Velocity Calculations	QC Process	Observation System	Spatial and Temporal Scale
Semiletov et al (2004)	Point Barrow, Alaska	Melting landfast sea ice	06/06/2002 to 24/06/2002	Land based tower	Unclear – could be either closed or open pathed	None described.	10 Hz using a three-dimensional sonic anemometer-thermometer (SWS-211/ 3K, Applied Technologies, inc., Boulder, CO)	If a closed-path CO_2 was used flux estimates were corrected for the simultaneous flux of H_20 vapor (Leuning and Moncrieff, 1990; Suyker and Verma, 1993),if open-path flux estimates were corrected for the simultaneous fluctuations in both heat and H_20 vapor (Webb et al., 1980) Transfer functions (Moore, 1986)to correct for high-frequency flux loss	k not calculated.	CO_2 fluxes were averaged to 30 minute windows.	N/A	N/A
Zemmelink et al. (2006)	Weddell Sea, Antarctica	37 day drift station on an ice floe in the Western Weddell Sea in the perennial ice zone.	November – December 2004	Tower mounted on a drift ice station	Open-path infrared CO_2/H_2O analyzer (Li-7500, Li-COR, USA)		SATI/3K three-axis sonic anemometer	Coordinate rotation Webb correction (Webb et al., 1980) for variations in CO_2 density due to heat and water vapour fluctuations.	k not calculated.	CO_2 fluxes were averaged to 30 minute windows.	Aerial Photography and Electromagnetic soundings	70 km along either side of the floe
Semiletov et al. (2007)	Arctic Shelf Slope	multi-year sea ice edge	September 2005	Ice-breaker “Kapitan Dranytsin”; ice-station	fast response open-path infrared Li-Cor 7500 gas analyzer. To	None	sonic thermo-anemometer (USA-1, METEC)	Flux estimates were corrected for the simultaneous fluctuations in both heat and H20 vapor (Webb et al., 1980). Transfer functions (Moore, 1986) to correct for high-frequency flux loss	k not calculated.	CO_2 fluxes were averaged to 30 minute windows.	N/A	N/A
Papkyriakou and Miller, 2011)	McDougall Sound, Canadian Archipelago	first-year sea ice in McDougall Sound approximately 3 km from the south-western coast of Truro Island	09/05/2002 to 24/06/2002	Tower mounted on ice	CSAT3 three-dimensional (3-D) ultrasonic anemometer (Campbell Scientific1, Logan, UT, USA) and	LI-7500 open-path gas analyzer (LI-COR1, Lincoln, NE, USA),		Coordinate rotation of the covariances (McMillen, 1988). Density corrections for the CO_2 flux, including the Webb correction (Webb et al. 1980) following (Massman and Lee, 2002). Correction for air density fluctuations in the gas analyser’s optical path associated with heating of the sensor itself (Burba, G. G. *et al.*, 2008).	k not calculated.	CO_2 fluxes were averaged to 15 minute windows which were rejected when: 1. Wind directions were between 270° and 300° (west-northwest), and between 350° to 10° (i.e., due north) to minimize possible impacts of the ship, the tower, and generator 2. Wind speeds were ‘excessively’ high or low 3. power interruptions occurred 4. sensors were covered with frost and rime	N/A	N/A

Study Overview					Eddy Covariance Equipment			Data Processing			Sea Ice Characterisation	
Study	Location	Description	Time of year	Platform	Gas Analysers	Air-Drying	Wind	Corrections	Gas Transfer Velocity Calculations	QC Process	Observation System	Spatial and Temporal Scale
Miller et al. (2011)	Southern Beaufort Sea, Arctic	Winter time series of air-sea CO_2 fluxes in an area of landfast sea ice	22/01/2004 to 25/05/2004	EC equipment mounted on an open TV antenna-type tower	LI-7500 LI-COR (open path)	None	Campbell Scientific CSAT3 sonic anemometer mounted facing 190º	Webb correction (Webb et al., 1980) for variations in CO_2 density due to heat and water vapour fluctuations. Correction for air density fluctuations in the gas analyser's optical path associated with heating of the sensor itself (Burba et al., 2008).	k not calculated.	CO_2 flux measurements were rejected when: 1. Wind directions were between 270° and 300° (west-northwest), and between 350° to 10° (i.e., due north) to minimize possible impacts of the ship, the tower, and generator 2. power interruptions occurred 3. sensors were covered with frost and rime	N/A	N/A
Else et al. (2011)	Amundsen Gulf, Canadian Arctic	Air-sea CO_2 fluxes collected in an active Arctic Polynya during transects and drifting stations as part of the the International Polar Year Circumpolar Flaw Lead Study (CFL)	01/11/2007 to 31/01/2008	IcebreakerCCGS Amundsen – Moving Vessel	LI-COR LI-7500 (open path)	None	Gill Windmaster Pro sonic anemometer	Webb correction (Webb et al., 1980) for variations in CO_2 density due to heat and water vapour fluctuations. Wind corrected for ships motion using MotionPak data Corrected for associated open path gas analyser errors using multivariate regression model for determining sensor heat flux from air temperature, wind velocity and incoming longwave/shortwave radiation as proposed by Burba et al., (2008)	k not calculated, but pCO_{2w} and ΔCO_2 calculated for comparison. pCO_{2w} measured using a LI-COR LI-7000 CO_2/H_2O gas analyser sampling from water measured by a continuous line at ~5 m depth	Averaged to 30 minute CO_2 flux intervals which were rejected when: 1. Significant changes in ship operation (greater than ±3.7 km hr^{-1} of mean for velocity and ±27.5° of mean for course) occurred 2. Significant changes in atmospheric conditions occurred. 3. Wind direction was greater than ±27.5° of the mean 4. Wind direction was greater than ±90° relative to the bow to eliminate winds affected by flow distortion from the boat 5. lens obstruction of LI-7500 occurred due to riming. To reduce impact of non-homogenous surfaces data was split into discrete case studies during which flux data collection was consistent, the ship location, atmospheric conditions and sea ice conditions were fairly uniform.	RADARSAT-1 ScanSAR narrow beam images	50 m, Daily

Study Overview					Eddy Covariance Equipment			Data Processing			Sea Ice Characterisation	
Study	Location	Description	Time of year	Platform	Gas Analysers	Air-Drying	Wind	Corrections	Flux/Gas Transfer Velocity Calculations	QC Process	Observation System	Spatial and Temporal Scale
Sørensen et al. (2014)	Greenlandic Fjord	Air-ice-sea fluxes of CO2 collected over later Winter.	12 - 16 March 2010 seasonal landfast ice	Ice mounted tower	LI-COR LI-7500 (open path)	None.	METEK USA-1 sonic anemometer	Density correction based on external measurements of temperature and pressure using the point-by-point method described by Sahlee et al. (2008),	K not calculated	Data set was filtered based on a careful inspection of spectra resulting in a set of data where the direction of the flux can be clearly identified from the cospectra	Ice and snow characteristics from ice cores. No spatial measurements of sea ice	Discrete samples, Sub-daily
Sievers et al. (2015)	Greenlandic Fjord	Air-sea fluxes of CO2 collected during winter over landfast sea ice (ICE1, DNB) and a polynya (POLY1)	20 – 27th March (ICE1) 29th March – 27th April (DNB), 25th to 27th March (POLY1).	Ice mounted stationary (ICE1) and mobile (POLY1, DNB) towers	LI-COR LI-7500 (open path) LI-COR LI-7200 (closed path)	None.	Gill Wind-master sonic (ICE1), METEK USA-1 sonic anemometer (POLY1, DNB)	Density correction based on external measurements of temperature and pressure using the point-by-point method described by Sahlee et al. (2008),	K not calculated	Surface flux estimates of CO2, sensible and latent heat were derived using ogive optimization (Sievers et al., 2015). Flux estimates were discarded only if an excessive number of gaps were present in the raw data set or if no theoretical model ogive distribution can be optimized sufficiently.	Ice and snow characteristics from ice cores. No spatial measurements of sea ice.	Discrete samples, Sub-daily
Butterworth and Miller (2016)	Southern Ocean and Antarctic MIZ (see figure)	Air-sea fluxes of CO_2 collected on two cruises through open water in the Southern Ocean and the Antarctic MIZ (NBP-1210 and NBP-1402)	NBP-1210: 01/01/2013 to 08/02/2013 NBP-1402: 29/01/2014 to 15/03/2014	RV Nathaniel B. Palmer - Moving Vessel	LI-COR LI-7500 (open path) LI-COR LI-7200 (closed path) LI-COR LI-7200 (closed path)	Inline Nafion air-drying system	Campbell Scientific CSAT3 sonic anemometer (2 x Bow mounted on port and starboard)	Webb correction (Webb et al., 1980) for variations in CO_2 density due to heat and water vapour fluctuations. Motion correction applied to CO_2 mixing ratios to eliminate spurious signals due to the physical movement of the IRGAs (Miller et al. 2010). Schotanus *et al.* (1983) correction for the effect of water vapour on air density and speed of sound. Wind vector motion correction for effect of moving platform (Miller et al., 2008)	Calculated k by rearranging the bulk flux equation (equation 1) using: 1. pCO_{2a} measured by the infrared gas analyser 2. pCO_{2w} measured at 5m depth by the underway system. 3. Airside/waterside CO_2 solubility k_{raw} was adjusted to a Schmidt number of 660, corresponding to sea surface temperature of 20°C.	Averaged to 10 minute CO_2 flux intervals which were rejected when: 1. Wind direction was greater than ±90° relative to the bow to eliminate winds affected by flow distortion from the boat 2. The magnitude of ΔpCO_2 was less than 40 uatm. Calculated k < -100 cmh-1 or greater than 200cmh-1 flagged as outliers. k_{miz} that were 10 times higher than k_{open} were removed as outliers.	Two mounted Campbell Scientific CC5MPX	Image Footprint - 3000 m² (approx 55 m x 55 m). Photos taken every second

Study Overview					Eddy Covariance Equipment			Data Processing			Sea Ice Characterisation	
Study	Location	Description	Time of year	Platform	Gas Analysers	Air-Drying	Wind	Corrections	Flux/Gas Transfer Velocity Calculations	QC Process	Observation System	Study Overview
Prytherch et al. (2017)	Arctic MIZ (see figure)	Collected across the Arctic basin during the ACSE cruise.	05/07/2014 to 05/10/2014	Icebreaker Oden - Moving Vessel	Los Gatos Fast Greenhouse Gas Analyser	None	Metek USA-1 sonic anemometer mounted on mast over Oden's bow	No correction for ship motion due to lack of co-located IMU with FGGA. Airflow model of ship (Moat et al., 2015) used to determine wind-direction-dependent corrections following Yelland et al., (2002). Due to no available capacity for instrument maintenance increasing uncertainty and eventual failure of the H_20 and CO_2 channels occurred. Corrections to CO_2 following H_20 failure applied according to Miller et al., (2010).	Calculated k by rearranging the bulk flux equation (equation 1) using: 1. pCO_{2w} measured using the Stockholm University Water Equilibration Gas Analyser System (WEGAS) (Thornton *et al.*, 2016) sampling from the underway system at 8 m depth and rosette bottles at 5 and 10 m depth at discrete stations. When the WEGAS system was unavailable bottle measurements were linearly interpolated to the flux-observation time with a maximum allowed time difference of 12 hours 2. pCO_{2a} measured by the Los Gatos FGGA. 3. Airside/waterside solubility used k was normalised to a Schmidt number of 660 with an exponent of 0.5 following Wanninkhof (2014).	Averaged to 20 minute CO_2 flux intervals which were rejected when: 1. Wind direction was greater than ±120° relative to the bow to eliminate winds affected by flow distortion from the boat 2. The magnitude of ΔpCO_2 was less than 40 ppm. 3. Turbulent statistics passed quality control following Foken and Wichura (1996)	Satellite Derived Passive Microwave Data from AMSR2 using the artist sea ice algorithm (ASI 5).	6.25 km x 6.25 km grid, 1 day
Butterworth and Else (2018)	Qikirtaarjuk Island, Dease Strait, Canadian Arctic	Air-sea CO_2 fluxes measured over landfast sea ice	4 May to 1 September 2017 (Spring melt season)	EC system installed on Qikirtaarjuk Island	Campbell Scientific EC150 (open path) LI-COR LI-7500 (open path) LI-COR LI-7200RS (closed path)	Nafion PD-200T-12MPS moisture exchanger with a dessicant (Du-Cal Drierite) to purge water vapour from the counterflow	3-D ultrasonic CSAT3 anemometer	Webb correction (Webb et al., 1980) for variations in CO_2 density due to heat and water vapour fluctuations. Schotanus et al. (1983) correction for the effect of water vapour on air density and speed of sound.	pCO_{2w} was not measured so gas transfer could not be calculated.	Averaged to 20 minute CO_2 flux intervals which were rejected when: 1. Intervals selected that exhibit stationarity to remove intervals with flux contributions from large-scale phenomena outside the frequency range of turbulent fluxes. 2. Wind directions greater than ±150 ° to eliminate winds affected by flow distortion from the tower.	Photos taken with a tower mounted (1) Go Pro Hero 4 and (2) Campbell Scientific CC5MPX, (3) Satellite Derived Passive Microwave Data from AMSR2 using the artist sea ice algorithm (ASI 5). (4) Landsat-8 and (5) MODIS images (5) Aerial photographs taken from a helicopter.	(1) unknown, hourly (2) unknown, every 5 minutes (3) 3.125 km grid, daily (4) 30 m, every 8 days dependent on when cloud cover permits (5) 250 m, 1-2 days dependent on when cloud cover permits (6) variable

Study Overview					Eddy Covariance Equipment			Data Processing			Sea Ice Characterisation	
Study	Location	Description	Time of year	Platform	Gas Analysers	Air-Drying	Wind	Corrections	Flux/Gas Transfer Velocity Calculations	QC Process	Observation System	Study Overview
Prytherch and Yelland (2021)	Central Arctic Ocean	Air-sea fluxes measured over a lead system within dense pack ice in the central Arctic Ocean	Late Summer to Early Autumn,	Drift station on ice floe, Central Arctic Ocean	Closed-path Li-Cor 7200 Open-path Li-Cor 7500	None	METEK uSonic-3 heated sonic anemometer	Sensible heat flux corrected for side wind path lengthening (van Dijk et al., 2004). Fast response H2O density measurements from the open-path IRGA are corrected for density effects (Webb et al., 1980) on a point-by-point basis following Miller et al. (2010; 2004). The Humidity is corrected for in the sensible heat flux calculation using a bulk estimate of the latent heat flux (Smith, 1988) following Persson et al. (2005). Fast	Calculated k by rearranging the bulk flux equation (equation 1) using: 1. Waterside CO_2 was measured at a depth of 0.5 m in the open lead using the CO_2-Pro CV membrane equilibration instrument. 2. pCO2a measured by the Li-Cor 7200 (Closed-path)	CO_2 fluxes were averaged to 30 minute windows. Standard statistical tests for skewness, kurtosis (Vickers and Mahrt, 1997) and stationarity (Foken and Wichura, 1996) were applied to assess the suitability of the measurements for flux calculation.	Spatial dimensions of lead measured using a hand-held laser range finder (Naturalife PF4)	metres, attempted twice daily.